Catalytic Microspheres

DOI: 10.1002/anie.201106948

A General Approach to Mesoporous Metal Oxide Microspheres Loaded with Noble Metal Nanoparticles**

*Zhao Jin, Manda Xiao, Zhihong Bao, Peng Wang, and Jianfang Wang**

Noble metal nanoparticles are widely used as catalysts in energy processing, chemical production, and pollution control.[1–4] They are usually dispersed finely on solid oxide supports to prevent agglomeration, particle growth, and therefore a decrease in the total surface area.[5] Moreover, metal oxide supports can also play important roles in catalytic reactions through synergistic interactions with loaded metal nanoparticles.[6–10] For example, bonding between Ti atoms of titania supports and Au atoms of Au nanoparticles can activate Au nanoparticle catalysts during CO oxidation.[11] In Pt–ceria-based water/gas-shift catalysts, nanostructured ceria supports boost the transport of activated oxygen from ceria to loaded Pt nanoparticles.[12] On the other hand, supported metal nanoparticles can enhance light absorption and charge-carrier separation in metal oxide semiconductors for photocatalytic applications.[13,14] In this regard, the design and preparation of more efficient, stable, and economical catalysts composed of oxides loaded with metal nanoparticles is a major direction in catalysis research.

Impregnation and coprecipitation are two major methods adopted for the industrial-scale preparation of oxide catalysts loaded with metal nanoparticles.[15] Besides industrial methods, sputtering,[16] hydrothermal reaction,[17] and sol–gel methods[18] have also been investigated experimentally. However, these methods either lack control of the support morphology or require complex preparation processes. In addition, when metal nanoparticles are loaded on mesoporous powder materials, either through metal salts or after prepreparation, diffusion of the metal species into the nanoscale pore channels is difficult, and nanoparticles adsorbed close to the pore openings can block further diffusion. Therefore, the amount and spatially uniform distribution of loaded metal nanoparticles are difficult to control.[19] A high-yield preparation route that is capable of producing oxide catalysts loaded with metal nanoparticles with high support surface areas and uniform nanoparticle distributions will therefore undoubtedly benefit the catalyst industry.

One promising strategy to this end is the aerosol-assisted self-assembly (AASA) process, which combines aerosol spraying and evaporation-induced assembly. The aerosol-spraying approach allows for continuous and easy mass production of microspheres with controllable compositions and ingredients. Previous preparations using AASA have mainly focused on mesoporous silica and metal oxide microspheres with high surface areas.[20–26] Incorporation of metal nanoparticles into these microspheres and their catalytic properties have not been systematically explored.

Herein we describe a simple, scalable preparation strategy for the production of diverse metal oxide microspheres loaded with metal nanoparticles as catalysts. Nine types of such microspheres have been prepared, including TiO_2, ZrO_2, Al_2O_3 microspheres as supports and Au, Pd, and Pt as nanoparticles. The mesoporous microspheres were prepared by a combination of acid-mediated sol–gel chemistry, where metal alkoxides are dissolved in mixed solutions of acetic acid, hydrochloric acid, and ethanol, with the AASA approach. The noble metal nanoparticles were readily incorporated into the microspheres by dissolving the corresponding metal salts in the precursor solutions and subjecting the sprayed products to thermal treatment or hydrogen reduction. In contrast to previous postloading methods, in our approach, incorporation of metal precursors and formation of mesostructured materials take place in one pot.

The loaded metal ions were uniformly distributed in the mesostructured oxide microspheres, and therefore the produced metal nanoparticles were also uniformly distributed. This allows for more efficient use of the support materials and can increase the encounter probability between reactant molecules and metal nanoparticles. The catalytic properties of the nanoparticle-loaded microspheres were systematically examined in a model reaction based on the reduction of 4-nitrophenol (4-NP) with sodium borohydride to 4-aminophenol (4-AP). The studies revealed that the catalytic efficiency varies with the type of metal nanoparticles for the same oxide support, with the type of metal oxide supports for the same type of metal nanoparticles, and with the loaded amount of metal nanoparticles. TiO_2 microspheres loaded with Au and Pd nanoparticles exhibited higher catalytic efficiencies than the other catalysts. Our results therefore provide a general approach for the preparation and discovery of high-performance oxide catalysts loaded with metal nanoparticles for various chemical reactions.

Figure 1 shows representative scanning electron microscopy (SEM) and transmission electron microscopy (TEM) images of the mesoporous oxide microspheres loaded with

[*] Z. Jin, M. D. Xiao, Dr. Z. H. Bao, Prof. J. F. Wang
Department of Physics, The Chinese University of Hong Kong
Shatin, Hong Kong SAR (P.R. China)
E-mail: jfwang@phy.cuhk.edu.hk
Prof. P. Wang
Water Desalination and Reuse Center
Chemical and Life Sciences & Engineering Division
King Abdullah University of Science and Technology
Thuwal (Saudi Arabia)

[**] This work was supported by the NSFC/RGC Joint Research Scheme (Ref. No.: N_CUHK465/09; Project Code: 2900339) and the Hong Kong RGC Direct Allocation (Project Code: 2060417).

Supporting information for this article is available on the WWW under http://dx.doi.org/10.1002/anie.201106948.

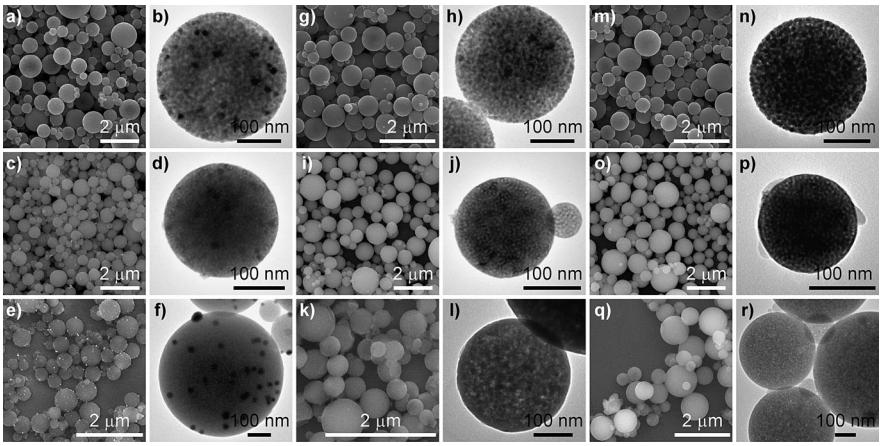

Figure 1. SEM (first, third, and fifth column) and TEM (second, fourth, and sixth column) images of the mesoporous metal oxide microspheres loaded with metal nanoparticles. a, b) TiO_2/Au. c, d) ZrO_2/Au. e, f) Al_2O_3/Au. g, h) TiO_2/Pd. i, j) ZrO_2/Pd. k, l) Al_2O_3/Pd. m, n) TiO_2/Pt. o, p) ZrO_2/Pt. q, r) Al_2O_3/Pt.

1 mol% of noble metal nanoparticles. The molar percentage of the loaded metal nanoparticles, which refers to the amount added during preparation, is defined relative to the number of moles of Ti, Zr, and Al, respectively, contained in the three types of oxides. The diameters of the microspheres range from 50 nm to 1 μm, and are very similar to those of microspheres prepared under the same conditions without addition of the metal salts (Figure S1, Supporting Information). Nitrogen adsorption measurements (Figure S2, Supporting Information) show that the TiO_2, ZrO_2, and Al_2O_3 microspheres are mesoporous. Their BET surface areas are 151, 186, and 160 m^2g^{-1}, respectively, and their Barrett–Joyner–Halenda (BJH) pore sizes, determined from the adsorption branches, are 7.7, 5.1, and 13.6 nm, respectively. The X-ray diffraction (XRD) patterns (Figure S3, Supporting Information) show that the pore walls of the mesoporous TiO_2 and ZrO_2 microspheres contain anatase titania and cubic zirconia nanocrystals, while those of the mesoporous Al_2O_3 microspheres are completely amorphous. The sizes of the titania and zirconia nanocrystals were estimated from the diffraction peak widths to be 10 and 7 nm, respectively.

The Au nanoparticles obtained after thermal treatment of the three types of oxide microspheres can be readily observed in TEM images (Figure 1 b,d,f). They are randomly distributed, and their sizes are in the range of 10–30 nm according to the TEM images. The crystalline nature of the loaded Au nanoparticles is also corroborated by the XRD patterns. Moreover, the nanocrystalline nature of the oxide pore walls is maintained after loading of the metal nanoparticles. Figure 2 a shows the XRD pattern of the TiO_2/0.5 mol% Au microspheres. The sizes of the crystalline TiO_2 and Au nanoparticles are estimated from their diffraction peak widths to be 9 and 10 nm, respectively. Figure 2 b shows the XRD pattern of the Al_2O_3/1 mol% Au microsphere sample. The estimated size of the Au nanoparticles is 19 nm. In contrast, the Pd and Pt nanoparticles in all of the three oxide supports are difficult to observe by TEM imaging (Figure 1 h,j,l,n,p,r) even though the microspheres were thermally treated with H_2. This suggests that the Pd and Pt nanoparticles in the oxide microspheres are very small. Such small sizes are consistent with the broad and weak diffraction peaks in the XRD patterns (Figure 2 c,d). Such a large difference in the formation behavior of the Au versus Pd and Pt nanoparticles in the oxide supports remains mysterious.

To ascertain whether the metal nanoparticles exist on the surface of or inside the oxide microspheres, we broke the Au loaded TiO_2 microspheres by gentle grinding and recorded SEM images in both secondary- and backscattered-electron modes (Figure 2 e,f). Because Au atoms are heavier than Ti and O atoms, the Au nanoparticles are brighter in the backscattered SEM images. A comparison of the SEM images recorded in the two modes indicates that the Au nanoparticles are present both on the surface of and inside the TiO_2 microspheres.

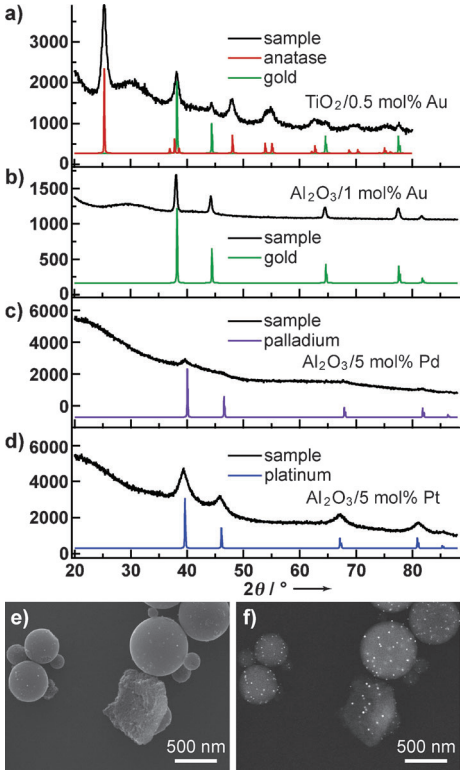

Figure 2. a-d) XRD patterns of the TiO_2/0.5 mol% Au, Al_2O_3/1 mol% Au, Al_2O_3/1 mol% Pd, and Al_2O_3/1 mol% Pt microspheres, respectively. The smooth, colored curves are the standard powder diffraction patterns of the corresponding materials. e, f) SEM images recorded from the same region of a broken TiO_2/1 mol% Au microsphere sample in secondary-electron and backscattered-electron modes, respectively.

The catalytic performance of the mesoporous oxide microspheres loaded with the noble metal nanoparticles was

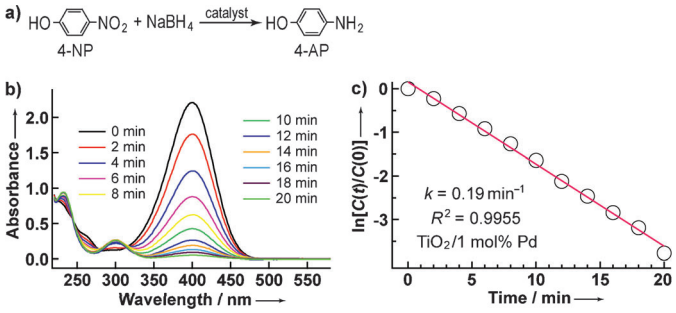

Figure 3. Catalytic reduction of 4-NP to 4-AP. a) Reaction equation. b) Time-dependent absorption spectra of the reaction solution in the presence of the TiO_2/1 mol% Pd microspheres. c) Plot of $\ln[C(t)/C(0)]$ against the reaction time.

quantitatively evaluated in the liquid-phase reduction of 4-NP by $NaBH_4$ (Figure 3a). The reaction is known to be catalytically accelerated in the presence of metal nanoparticles at room temperature.[27–29] 4-NP exhibits an absorption peak at 317 nm in neutral or acidic solution. The addition of $NaBH_4$ deprotonates the OH group of 4-NP, and the absorption peak shifts to 400 nm.[30,31] When the reduction of 4-NP is started, the absorption peak at 400 nm gradually drops in intensity. Meanwhile, a small shoulder at 300 nm gradually rises, which is attributed to absorption of 4-AP. The reaction process can therefore be monitored by recording the absorption spectra of the reaction solution as a function of reaction time. Loading amounts of 0.1 and 1 mol% for the metal nanoparticles were tested for each microsphere sample. A total of 18 samples were examined.

Figure 3b, as an example, shows the time-dependent absorption spectra of the reaction solution with TiO_2/1 mol% Pd microspheres as catalyst. The absorption peak at 400 nm drops gradually in intensity and nearly disappears 20 min after the addition of the catalyst, which suggests that the reaction is complete. Because $NaBH_4$ is in great excess in the reaction, its concentration can be regarded as being constant throughout the reaction. Therefore, pseudo-first-order kinetics can be applied with respect to 4-NP. Figure 3c shows the plot of $\ln[C(t)/C(0)]$ against reaction time, where $C(t)$ and $C(0)$ are the concentrations of 4-NP at time t and 0, respectively. They were converted from the peak absorbances at 400 nm according to the predetermined calibration curve (Figure S4, Supporting Information). The linear fit with a coefficient of determination very close to unity also supports the assumption of pseudo-first-order kinetics.

The reaction rate constant k, calculated from the rate equation $\ln[C(t)/C(0)] = kt$, is 0.19 min^{-1} for the TiO_2 microspheres loaded with 1 mol% Pd nanoparticles. The reaction kinetics and rate constants of the other 17 catalyst samples are shown in Figures S5–S7 of the Supporting Information. All reactions exhibit pseudo-first-order kinetics. In comparison, the reduction of 4-NP with the three pure oxide microsphere samples as catalysts results in less than 10% decrease in peak absorbance after 1 h (Figure S8, Supporting Information). The decrease in absorbance is attributed to adsorption of 4-NP molecules on the precipitated mesoporous oxide microspheres. The pure mesoporous oxide microspheres alone cannot catalyze the reduction of 4-NP.

The turnover frequency (TOF), defined as the moles of reduced 4-NP molecules per mole of noble metal atoms in the oxide microspheres per minute, was used to compare the overall catalytic performances of the different microsphere samples (Figure 4 and Table S1, Supporting Information). First, the TOFs vary from 0.4 (for the TiO_2/0.1 mol% Pd microspheres) to 97 min^{-1} (for the Al_2O_3/1 mol% Pt microspheres). Pd nanoparticles are catalytically active on all three oxide supports, while Au nanoparticles only show catalytic activities on the TiO_2 microspheres. The catalytic performance of Pt nanoparticles is poor in all three types of oxide microspheres. Our finding that Pd nanoparticles exhibit the highest catalytic activities is in agreement with previous studies.[32,33]

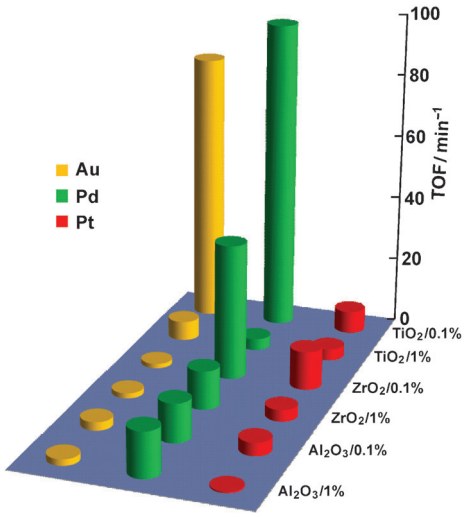

Figure 4. TOFs of the different microsphere samples.

Second, a 0.1 mol% loading of metal nanoparticles generally leads to higher TOFs than a loading of 1 mol%. This is because the metal nanoparticles are generally smaller at lower loadings, as evidenced by TEM (Figure S9, Supporting Information) and XRD measurements. Smaller noble metal nanoparticles have higher fractions of coordinatively unsaturated surface atoms, which are highly catalytically active. In addition, the total surface areas of smaller metal nanoparticles will be higher at the same weight. Therefore, smaller metal nanoparticles exhibit higher catalytic activity toward reduction of nitro compounds, as was also shown previously.[34,35]

Third, we calcined the TiO_2/0.1 mol% Pd, ZrO_2/0.1 mol% Pt, and Al_2O_3/0.1 mol% Pd microspheres at 700 °C to increase the degree of crystallization of the oxides.[24,25] Pd and Pt were chosen because the formation of Pd and Pt nanoparticles in the oxide microspheres is mainly determined by hydrogen treatment, while that of Au nanoparticles is highly sensitive to the thermal-treatment temperature. The TOF of the TiO_2/0.1 mol% Pd sample calcined at 700 °C drops by about 30% in comparison to that calcined at 400 °C, and the TOFs of the

ZrO_2/0.1 mol% Pt and Al_2O_3/0.1 mol% Pd samples stay nearly unchanged (Table S2, Supporting Information). The decreased TOF can be ascribed to the deterioration of the mesopores and partial blocking of the diffusion routes of the reactant molecules to the metal nanoparticles in the TiO_2 microspheres (Figure S10, Supporting Information). These results suggest that increasing the degree of crystallization of the oxide microspheres does not benefit the catalytic activity of the supported metal nanoparticles. On the other hand, because of the complex nature of the interactions among the loaded metal nanoparticles, the mesoporous oxide supports, and the reactant molecules, a complete understanding of the different catalytic performances of the microspheres remains challenging. However, our facile approach for the preparation of mesoporous oxide microspheres loaded with metal nanoparticles will be of great potential in discovering high-performance catalysts for various industrially important reactions.

Recyclability of catalysts is important for their practical application. To test the recyclability of our catalysts, four successive cycles of catalytic reduction were carried out with the TiO_2/0.1 mol% Au microspheres (Figure S11, Supporting Information). In the first three cycles, reduction of more than 70% 4-NP was complete within 10 min, but in the fourth run, only 35% 4-NP reacted within 10 min. The main reasons for decreases in catalytic performance are usually loss of catalyst during separation and reduced catalytic activity resulting from the reshaping and/or aggregation of metal nanoparticles. In each run of our experiments, the microspheres were precipitated by centrifugation, the supernatant was removed, and fresh reactant solution was added. In addition, small amounts of the reaction solution were taken for measuring the absorption spectra. We therefore believe that loss of microspheres is the main reason for the reduced catalytic performance, although morphological changes of the metal nanoparticles cannot be completely excluded.

In summary, we have demonstrated a general and facile approach for the preparation of mesoporous oxide microspheres loaded with noble metal nanoparticles by combining aerosol spraying and solvent-evaporation-induced assembly. The types of incorporated metal nanoparticles and the oxide supports can be readily varied by choosing different precursors. The loaded nanoparticles are distributed inside the entire oxide microspheres, and the mesoporous structure of the oxide microspheres allows access of molecular species in solution to the surfaces of the loaded nanoparticles. The catalytic performance of the loaded microspheres was quantitatively evaluated in the reduction of 4-NP by $NaBH_4$. The TiO_2/0.1 mol% Pd microspheres were found to exhibit the highest catalytic activity. We are currently expanding our approach to the preparation of other noble metals and oxide supports. Our method for continuous production of mesoporous oxide microspheres loaded with noble metal nanoparticles will be useful for discovering low-cost, highly efficient catalysts for industrially important chemical reactions.

Experimental Section

The preparation of the oxide microspheres has been reported before.[24] To prepare the TiO_2 microspheres, a mixture of titanium ethoxide (1 mL) and HCl (37 wt%, 3.2 mL) was first stirred for 2 h, and then added to a solution made by dissolving triblock copolymer (ethylene oxide)$_{106}$–(propylene oxide)$_{70}$–(ethylene oxide)$_{106}$ (F127, 0.6 g) in absolute ethanol (55.4 g). After stirring for one more hour, the solution was transferred to a household ultrasonic humidifier (1.7 MHz, 30 W) for the aerosol-spraying process. For the preparation of the ZrO_2 and Al_2O_3 microspheres, acetic acid was added to facilitate control of the hydrolysis and condensation of the oxide precursors. The molar ratios of the components in the precursor solutions were 1 $Zr(OBu)_4$:4 acetic acid:2.4 HCl:100 EtOH:0.01 F127 and 1 $Al(OBu)_3$:4 acetic acid:2.4 HCl:100 EtOH:0.01 F127. The mixed solutions were stirred for 3 h and then transferred into the ultrasonic humidifier. The generated mist was carried by N_2 into a glass tube in a 90 cm long tube furnace set at 380 °C. The produced oxide microspheres were collected on a filter connected to a water aspirator and then heat-treated at 400 °C for 4 h in air at a heating rate of 1 °C·min^{-1}. Preparation of the noble metal loaded oxide microspheres started with the same precursor solutions. An appropriate amount of noble metal salt ($HAuCl_4$, H_2PdCl_4, or H_2PtCl_6) was dissolved into the precursor solution. After calcination, the Pt- and Pd-loaded oxide microspheres were further treated at 350 °C for 2 h in flowing H_2/N_2 (5/95 v/v) at a heating rate of 5 °C min^{-1} to facilitate formation of Pt and Pd nanoparticles.

For catalytic reduction of 4-NP, aqueous solutions of 4-NP (0.01 M, 0.03 mL) and $NaBH_4$ (0.5 M, 0.2 mL) were mixed with water (2.5 mL) in a quartz cuvette with stirring. A sample of catalytic microspheres was dispersed in water in advance. The net weight of the catalyst sample in the reaction solution was in the range of 0.02–0.7 mg. After the catalyst dispersion was added, the reaction solution was stirred for 30 s and then the cuvette was transferred into a spectrophotometer. The reaction progress, without stirring, was monitored by taking absorption spectra. For testing the recyclability, the reaction solution was composed of 4-NP (0.1 M, 0.3 mL), $NaBH_4$ (0.5 M, 0.3 mL), and TiO_2/0.1 mol% Au catalyst (1 wt%, 0.2 mL). The reaction progress was monitored by taking out 0.02 mL of the solution at 4 min intervals, diluting it with water, and measuring the absorption spectrum. At the end of each cycle, the catalyst microspheres were precipitated by centrifugation and redispersed in a fresh mixture of the reactants.

Received: September 30, 2011
Revised: March 28, 2012
Published online: April 26, 2012

Keywords: aerosol spraying · mesoporous materials · metal oxides · microspheres · nanoparticles

[1] V. R. Stamenkovic, B. Fowler, B. S. Mun, G. F. Wang, P. N. Ross, C. A. Lucas, N. M. Marković, *Science* **2007**, *315*, 493 – 497.
[2] Y. P. Zhai, D. Pierre, R. Si, W. L. Deng, P. Ferrin, A. U. Nilekar, G. W. Peng, J. A. Herron, D. C. Bell, H. Saltsburg, M. Mavrikakis, M. Flytzani-Stephanopoulos, *Science* **2010**, *329*, 1633 – 1636.
[3] M. J. Climent, A. Corma, S. Iborra, *Chem. Rev.* **2011**, *111*, 1072 – 1133.
[4] Y. Nishihata, J. Mizuki, T. Akao, H. Tanaka, M. Uenishi, M. Kimura, T. Okamoto, N. Hamada, *Nature* **2002**, *418*, 164 – 167.
[5] S. H. Joo, J. Y. Park, C.-K. Tsung, Y. Yamada, P. D. Yang, G. A. Somorjai, *Nat. Mater.* **2009**, *8*, 126 – 131.
[6] A. Corma, P. Serna, *Science* **2006**, *313*, 332 – 334.
[7] D. I. Enache, J. K. Edwards, P. Landon, B. Solsona-Espriu, A. F. Carley, A. A. Herzing, M. Watanabe, C. J. Kiely, D. W. Knight, G. J. Hutchings, *Science* **2006**, *311*, 362 – 365.

[8] J. K. Edwards, E. Ntainjua N, A. F. Carley, A. A. Herzing, C. J. Kiely, G. J. Hutchings, *Angew. Chem.* **2009**, *121*, 8664 – 8667; *Angew. Chem. Int. Ed.* **2009**, *48*, 8512 – 8515.
[9] J. K. Edwards, B. Solsona, E. Ntainjua N, A. F. Carley, A. A. Herzing, C. J. Kiely, G. J. Hutchings, *Science* **2009**, *323*, 1037 – 1041.
[10] J. H. Kwak, J. Z. Hu, D. H. Mei, C.-W. Yi, D. H. Kim, C. H. F. Peden, L. F. Allard, J. Szanyi, *Science* **2009**, *325*, 1670 – 1673.
[11] M. S. Chen, D. W. Goodman, *Science* **2004**, *306*, 252 – 255.
[12] G. N. Vayssilov, Y. Lykhach, A. Migani, T. Staudt, G. P. Petrova, N. Tsud, T. Skála, A. Bruix, F. Illas, K. C. Prince, V. Matolín, K. M. Neyman, J. Libuda, *Nat. Mater.* **2011**, *10*, 310 – 315.
[13] T. Hirakawa, P. V. Kamat, *J. Am. Chem. Soc.* **2005**, *127*, 3928 – 3934.
[14] R. Costi, A. E. Saunders, E. Elmalem, A. Salant, U. Banin, *Nano Lett.* **2008**, *8*, 637 – 641.
[15] J. Hagen, *Industrial Catalysis*: *A Practical Approach*, Wiley-VCH, Weinheim, **2006**, pp. 223 – 237.
[16] S. H. Kang, Y.-E. Sung, W. H. Smyrl, *J. Electrochem. Soc.* **2008**, *155*, B1128 – B1135.
[17] R. M. Rioux, H. Song, M. Grass, S. Habas, K. Niesz, J. D. Hoefelmeyer, P. Yang, G. A. Somorjai, *Top. Catal.* **2006**, *39*, 167 – 174.
[18] B. Heinrichs, P. Delhez, J.-P. Schoebrechts, J.-P. Pirard, *J. Catal.* **1997**, *172*, 322 – 335.
[19] Z. Kónya, V. F. Puntes, I. Kiricsi, J. Zhu, J. W. Ager III, M. K. Ko, H. Frei, P. Alivisatos, G. A. Somorjai, *Chem. Mater.* **2003**, *15*, 1242 – 1248.
[20] Y. F. Lu, H. Y. Fan, A. Stump, T. L. Ward, T. Rieker, C. J. Brinker, *Nature* **1999**, *398*, 223 – 226.
[21] G. V. R. Rao, G. P. López, J. Bravo, H. Pham, A. K. Datye, H. F. Xu, T. L. Ward, *Adv. Mater.* **2002**, *14*, 1301 – 1304.
[22] X. M. Jiang, C. J. Brinker, *J. Am. Chem. Soc.* **2006**, *128*, 4512 – 4513.
[23] D. Grosso, G. J. de A. A. Soler Illia, E. L. Crepaldi, B. Charleux, C. Sanchez, *Adv. Funct. Mater.* **2003**, *13*, 37 – 42.
[24] C.-K. Tsung, J. Fan, N. F. Zheng, Q. H. Shi, A. J. Forman, J. F. Wang, G. D. Stucky, *Angew. Chem.* **2008**, *120*, 8810 – 8814; *Angew. Chem. Int. Ed.* **2008**, *47*, 8682 – 8686.
[25] L. Li, C.-K. Tsung, Z. Yang, G. D. Stucky, L. D. Sun, J. F. Wang, C. H. Yan, *Adv. Mater.* **2008**, *20*, 903 – 908.
[26] L. Li, C.-K. Tsung, T. Ming, Z. H. Sun, W. H. Ni, Q. H. Shi, G. D. Stucky, *Adv. Funct. Mater.* **2008**, *18*, 2956 – 2962.
[27] J. Lee, J. C. Park, H. Song, *Adv. Mater.* **2008**, *20*, 1523 – 1528.
[28] J. P. Ge, Q. Zhang, T. R. Zhang, Y. D. Yin, *Angew. Chem.* **2008**, *120*, 9056 – 9060; *Angew. Chem. Int. Ed.* **2008**, *47*, 8924 – 8928.
[29] J. Zeng, Q. Zhang, J. Y. Chen, Y. N. Xia, *Nano Lett.* **2010**, *10*, 30 – 35.
[30] K. Hayakawa, T. Yoshimura, K. Esumi, *Langmuir* **2003**, *19*, 5517 – 5521.
[31] S. Praharaj, S. Nath, S. K. Ghosh, S. Kundu, T. Pal, *Langmuir* **2004**, *20*, 9889 – 9892.
[32] Y. Lu, Y. Mei, M. Schrinner, M. Ballauff, M. W. Möller, J. Breu, *J. Phys. Chem. C* **2007**, *111*, 7676 – 7681.
[33] S.-D. Oh, M.-R. Kim, S.-H. Choi, J.-H. Chun, K.-P. Lee, A. Gopalan, C.-G. Hwang, K. Sang-Ho, O. J. Hoon, *J. Ind. Eng. Chem.* **2008**, *14*, 687 – 692.
[34] S. Panigrahi, S. Basu, S. Praharaj, S. Pande, S. Jana, A. Pal, S. K. Ghosh, T. Pal, *J. Phys. Chem. C* **2007**, *111*, 4596 – 4605.
[35] S. Wunder, F. Polzer, Y. Lu, Y. Mei, M. Ballauff, *J. Phys. Chem. C* **2010**, *114*, 8814 – 8820.

